

LASER INTERFEROMETER GRAVITATIONAL WAVE OBSERVATORY
- LIGO -
CALIFORNIA INSTITUTE OF TECHNOLOGY
MASSACHUSETTS INSTITUTE OF TECHNOLOGY

Technical Note

LIGO-T1800077-v3

2018/05/02

**Optimal control of the ARM
alignment with digital
compensation of the
Sidles-Sigg radiation torque**

Denis Martynov, Hang Yu, Lee McCuller
MIT

California Institute of Technology
LIGO Project, MS 100-36
Pasadena, CA 91125
Phone (626) 395-2129
Fax (626) 304-9834
E-mail: info@ligo.caltech.edu

Massachusetts Institute of Technology
LIGO Project, NW22-295
Cambridge, MA 02139
Phone (617) 253-4824
Fax (617) 253-7014
E-mail: info@ligo.mit.edu

LIGO Hanford Observatory
PO Box 159
Richland, WA 99352
Phone (509) 372-8106
Fax (509) 372-8137
E-mail: info@ligo.caltech.edu

LIGO Livingston Observatory
19100 LIGO Lane
Livingston, LA 70754
Phone (225) 686-3100
Fax (225) 686-7189
E-mail: info@ligo.caltech.edu

<http://www.ligo.caltech.edu/>

1 INTRODUCTION

The Sidles-Sigg (SS) radiation pressure torque is one of the limiting constraints for aLIGO high-power operation. This effect itself dramatically complicates the lock-acquisition procedure at different power levels, and the control servos to suppress it may inject a significant amount of sensing noise which contaminates the detector sensitivity below 30 Hz.

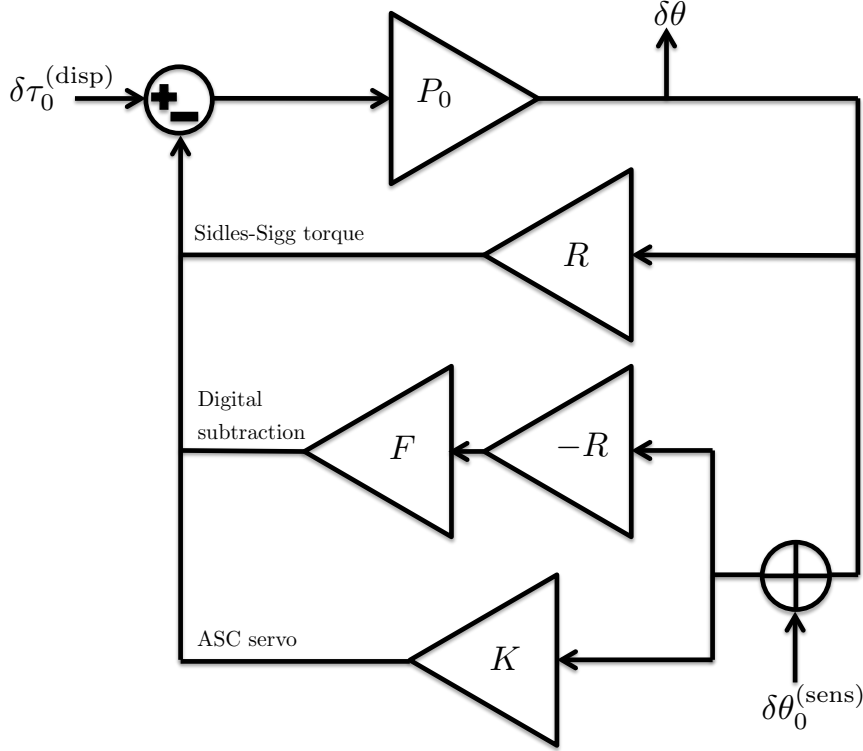


Figure 1: Signal flow diagram. In addition to the ASC control servo, we add a new digital path to (partially) compensate for the Sidles-Sigg effect.

Here we propose to apply the optimal control theory (namely, the H_∞ -synthesis and μ -synthesis) to stabilize the arm alignment. Furthermore, the control scheme can be combined with a digital compensation path to cancel the SS torque via feeding-forward. The scheme is illustrated in Fig. 1. In the figure, we use

- P_0 = Free pendulum torque to angle transfer function in [rad / N·m],
- R = The SS radiation torque per misaligned angle in [N·m / rad],
- F = Controller to turn on or off the digital compensator, dimensionless,
- K = Optimal controller designed with μ -synthesis in [N·m / rad].

Further, the SS torque per angle can be written as

$$R = -\frac{2P_{\text{arm}}}{c} \frac{dy}{d\theta}, \quad (1)$$

with P_{arm} the power circulating in the arms, c the speed of light, and $dy/d\theta$ the eigenvalues of the matrix $d\mathbf{Y}/d\Theta$. In the (θ_e, θ_i) basis, we have

$$\frac{d\mathbf{Y}}{d\Theta} = \frac{-L}{g_e g_i - 1} \begin{pmatrix} g_i & 1 \\ 1 & g_e \end{pmatrix}. \quad (2)$$

The eigenvectors of this matrix corresponds to the soft $[(\theta_e, \theta_i) = (1, 1.15)]$ and hard modes $[(\theta_e, \theta_i) = (1, -0.87)]$, and numerically the eigenvalues are

$$\left. \frac{dy}{d\theta} \right|_s = 2.07 \times 10^3 \frac{\text{m}}{\text{rad}}, \quad (3)$$

$$\left. \frac{dy}{d\theta} \right|_h = -4.55 \times 10^4 \frac{\text{m}}{\text{rad}}. \quad (4)$$

In this note we will show that with optimal control we can simultaneously improve the suppression of the low-frequency displacement noise to reduce the rms angular motion, and the roll-off of the high-frequency sensing noise to achieve better sensitivity to gravitational waves. The robustness of the control filters are examined in detail under the small gain theorem.

2 NOISE INPUT

Here we consider both the sensing noise and the displacement noise. From Fig. 1 it is easy to show that the physical angular motion induced by each kind of noise follows

$$\delta\theta^{(\text{sens})} = \frac{P_0 (FR - K)}{1 + P_0 (R - FR + K)} \delta\theta_0^{(\text{sens})}, \quad (5)$$

$$\begin{aligned} \delta\theta^{(\text{disp})} &= \frac{P_0}{1 + P_0 (R - FR + K)} \delta\tau_0^{(\text{disp})}, \\ &= \frac{1}{1 + P_0 (R - FR + K)} \delta\theta_0^{(\text{disp})}, \end{aligned} \quad (6)$$

where for the noise terms, we have used the subscript “0” to denote the input noise, and $\delta\theta_0^{(\text{disp})} \equiv P_0 \delta\tau_0^{(\text{disp})}$. For future convenience, we further define

$$OL = P_0 (R - FR + K) \quad (7)$$

as the open-loop transfer function. Note that when $F = 1$, i.e., we subtract out the radiation torque, $OL = P_0 K$, as one would expect.

The input displacement noise $\delta\theta_0^{(\text{disp})} = P_0 \delta\tau_0^{(\text{disp})}$ is shown in Fig. 2. Here we consider both the seismic noise and the damping noise, and assume that it is the same for the soft and hard modes.¹

For the sensing noise, we assume it to be a white noise with $\delta\theta_0^{(\text{sens})} = 5 \times 10^{-15} \text{ rad}/\sqrt{\text{Hz}}$. This is typical for the hard modes, and can be achieved for the soft mode if we use the AC-coupled DC QPD signal in the $> 0.01 \text{ Hz}$ band.

¹Note that when no control is implemented, the input noise in angular motion (in [rad]) depends on the power in the arm P_{arm} , as $\delta\theta^{(\text{disp})}(P_{\text{arm}}) = P_0 \delta\tau_0^{(\text{disp})} / [1 + P_0 R(P_{\text{arm}})] = P_{\text{ss}}(P_{\text{arm}}) \delta\tau_0^{(\text{disp})}$, with $P_{\text{ss}} = P_0 / [1 + P_0 R(P_{\text{arm}})]$. In the figure, we show $\delta\theta_0^{(\text{disp})} = \delta\theta^{(\text{disp})}(P_{\text{arm}} = 0)$.

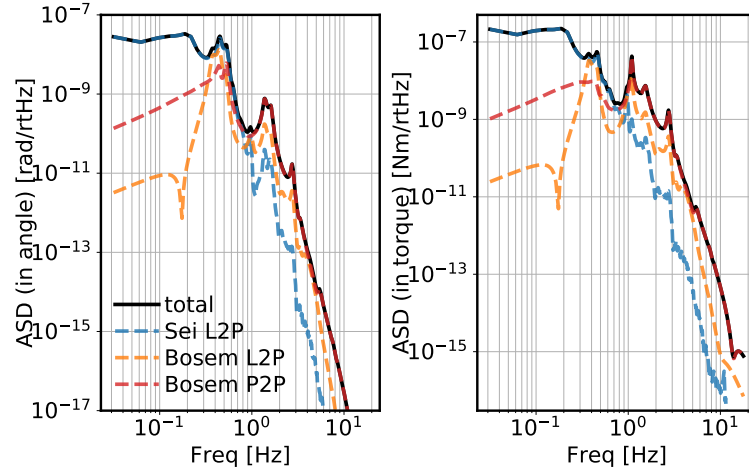


Figure 2: Input displacement noise $\delta\theta_0^{(\text{disp})}$ (left; evaluated at 0 arm power) and $\delta\tau_0^{(\text{disp})}$ (right) used in our calculations. It includes both the seismic motion and the sensing noise of the suspension damping loops.

3 SOFT MDOE

We consider the soft mode control with the digital compensation path on, $F_s = 1$. No extra lowpass is required as the sensing noise injected in this path is sufficiently low even when aLIGO reaches the full power with $P_{\text{arm}} = 0.75 \text{ MW}$. We thus have an essentially power-independent plant. We then perform the H_∞ -synthesis on the plant to obtain the optimal control filter².

The resultant open loop transfer function $OL_s = P_0 [K_s + (1 - F_s)R_s] = P_0 K_s$ is shown in Fig. 3. The blue trace is the result based on the optimal control design and the orange is a reference which should be a typical representation of the O1 configuration (it has an $1/f$ shape and a $UGF \simeq 3 \text{ Hz}$; there is extra roll-off starting at 8 Hz).

The OL can be translated into a noise performance, and result is shown in Fig. 4. Compared to the reference, the μ -synthesis result provides the same amount of loop suppression around the microseismic peak $\simeq 0.5 \text{ Hz}$ (the total rms is about the same), yet much better roll-off of the sensing noise at 10 Hz.

The noise budget is derived in the nominal case with $F_s = 1$, i.e., a perfect subtraction of the SS torque. In reality, however, imperfect subtraction may occur and the gain in the subtraction path may be set to $F_{s,\text{real}} = 1 + \Delta F_s$. This may potentially destabilize the loop if the gain mismatch $|\Delta F_s|$ is too large. Nevertheless, a *conservative* tolerance on ΔF_s can be derived based on the small gain theorem. We show in Fig. 5 the tolerance on subtraction gain mismatch for the case of $P_{\text{arm}} = 0.75 \text{ MW}$; the tolerance is greater for lower arm power.

²Actually a μ -synthesis is performed as we allow some imperfection in the digital subtraction.

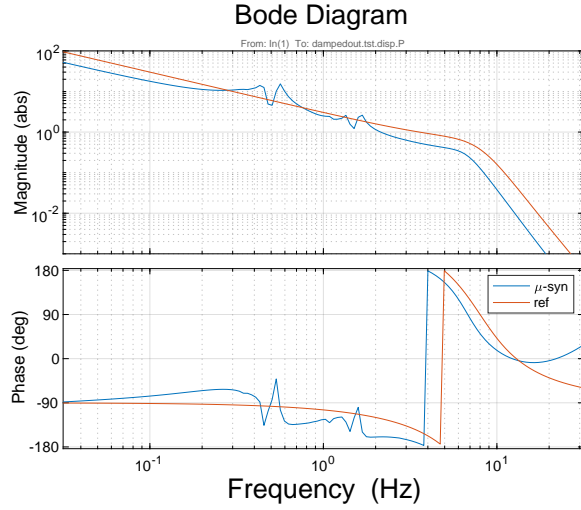


Figure 3: The open-loop transfer function for the soft mode. The blue line is the optimal control result and the orange one is a reference control configuration.

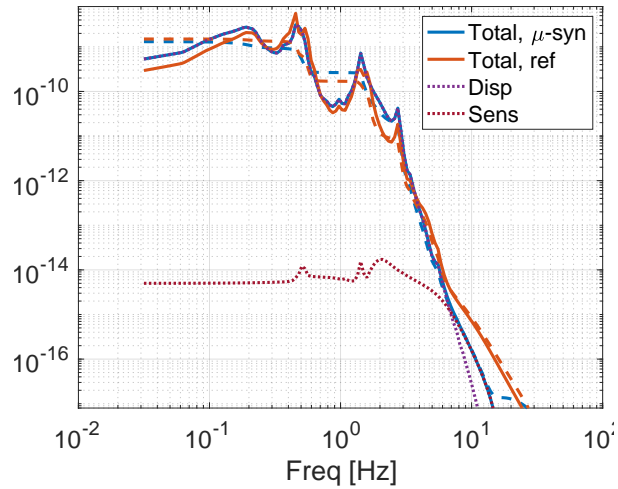


Figure 4: Noise budget for the soft mode. The solid lines are the total noise (blue for the μ -synthesis result and orange for the reference OL). The dashed lines are the cumulative rms. For the optimal control result, we also show its displacement and sensing noises in the dotted lines.

4 HARD MODE

For the hard mode, subtraction of the SS torque appears to be challenging. This is because the SS torque feedback for the hard mode, $P_0 R_h$, is large and extra lowpass would be necessary to avoid injecting sensing noise to the sensitivity band, yet the phase delay caused by the lowpass would make the subtraction imperfect, and the residual could still modify the plant. On the other hand, since the hard mode torque actually tends to stabilize the

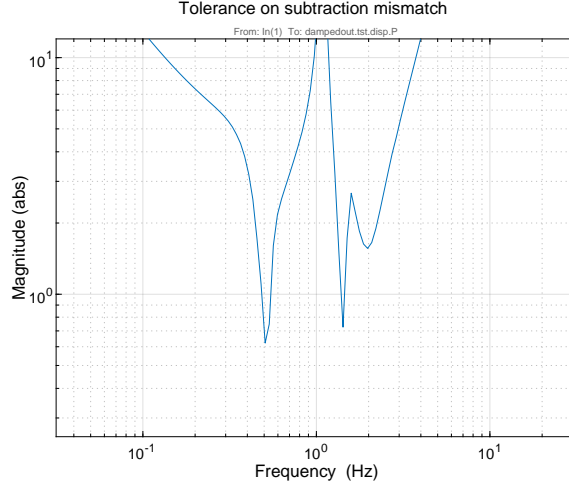


Figure 5: Tolerance on the subtraction gain mismatch $|\Delta F_s|$, assuming we use the optimally designed controller and the power circulating in the arm is 0.75 MW. For a given perturbation with $|\Delta F_s| <$ the minimum of the curve, it satisfies the *sufficient* condition of stability of the perturbed plant. Therefore, the curve serves only as a *conservative* estimation of the tolerance. It indicates that at least 60% DC gain mismatch in the subtraction path can be tolerated.

plant, we will design the optimal controller with the SS torque modified plant (i.e. $F_h = 0$). This means that our controller will depend on the arm power. Here we focus on the case where $P_{\text{arm}} = 0.75$ MW; the controller can be easily designed under the same principle for any other level of arm power.

In Fig. 6 we plot the open-loop transfer function $OL_h = P_0(K_h + R_h)$ for the hard mode. Note that because of the radiation torque feedback, the closed-loop sensing noise is not $OL_h/(1+OL_h)$, but instead, it should be evaluated according to Eq. (5) with $F_h = 0$ (i.e. no digital compensation). The closed-loop torque to angle transfer function and the closed-loop sensing noise roll-off are shown in Fig. 7.

The noise budget for the hard mode is shown in Fig. 8. Once again we see that the optimal control design improves both the low frequency rms and high frequency sensing noise compared to the reference configuration.

To study the robustness, we consider two types of perturbations. First, we consider the case where the power in the arm deviates from the nominal case by dP_{arm} . Via the SS mechanism, it causes an extra torque-to-torque feedback with gain of $[(dP_{\text{arm}}/P_{\text{arm}})R_hP_0]$. Second, we allow the controller DC gain to drift by $dK|_{(\text{DC})}$. This accounts for the possible drift in the sensing gain during a long lock stretch, which perturbs the torque-to-torque feedback from the ASC control by $[(dK/K)|_{(\text{DC})}KP_0]$. We can then use the small gain theorem to estimate conservative tolerances on the power fluctuation and control gain drift. This result is summarized in Fig. 9. It suggests that the loop will be stable for power drifts less than 30%, and for sensing gain drifts less than 45%.

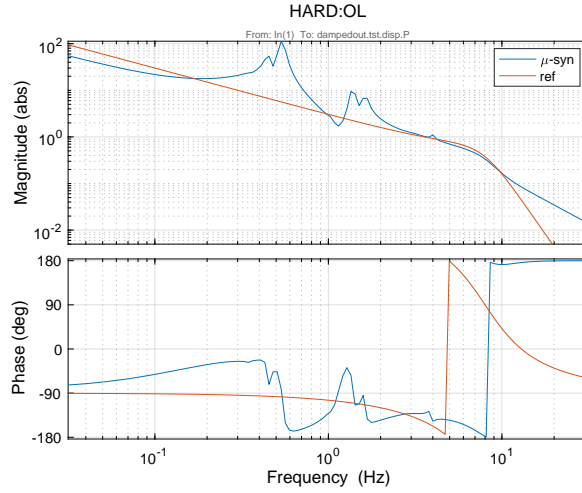
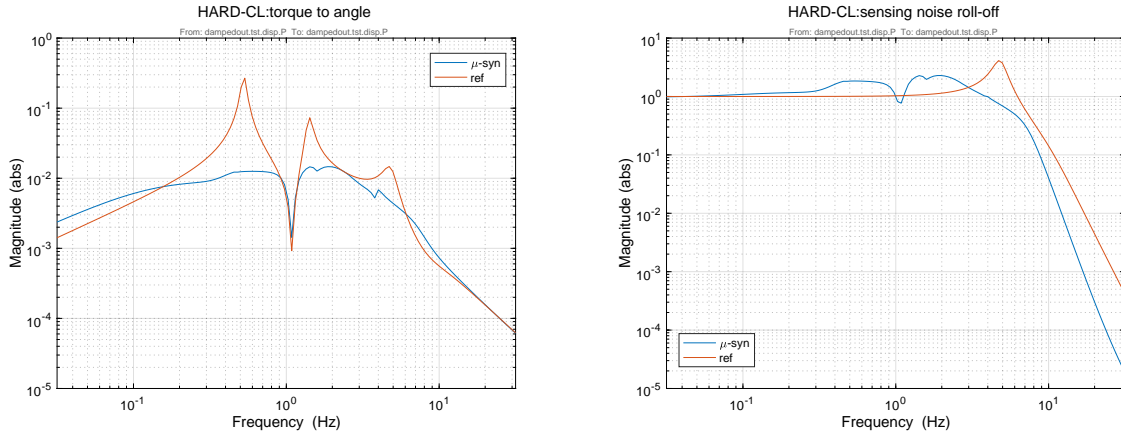


Figure 6: The open-loop transfer function, $OL_h = P_0(K_h + R_h)$, for the hard mode. The blue curve is the optimal controller designed with μ -synthesis and the orange one is the same reference we used in Fig. 3.



(a) Torque to angle in $[\text{rad}/\text{N} \cdot \text{m}]$.

(b) Roll off of the sensing noise in $[\text{rad}/\text{rad}]$.

Figure 7: Closed-loop responses for the hard loop.

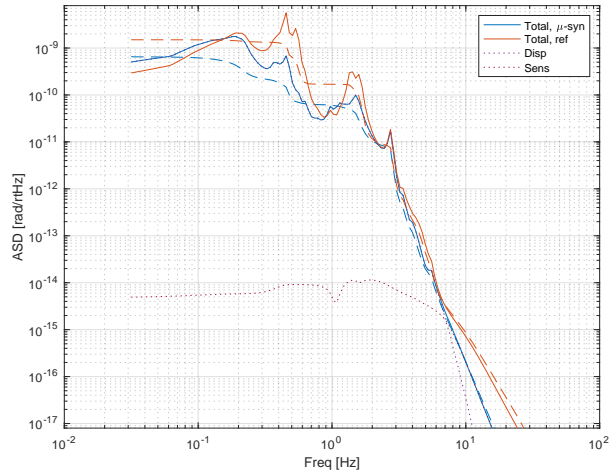
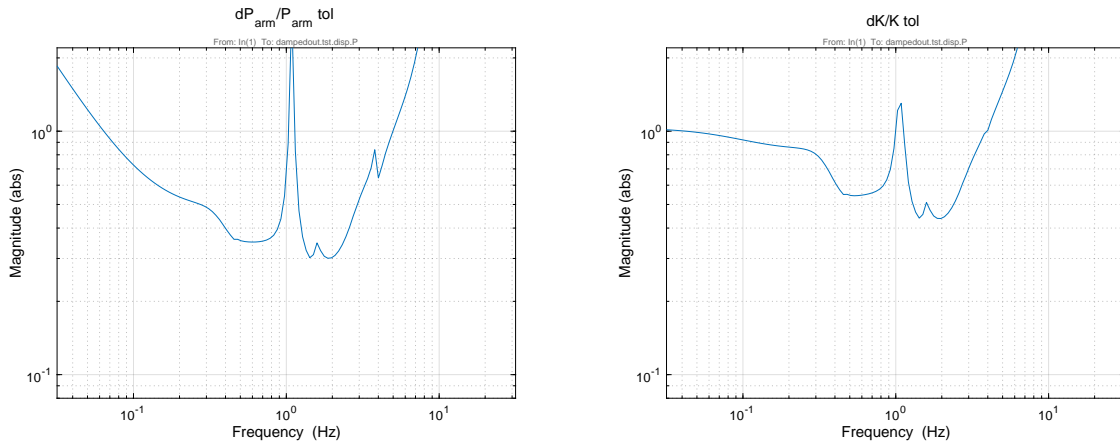


Figure 8: Noise budget for the hard mode. The solid lines are the total noise (blue for the μ -synthesis result and orange for the reference OL). The dashed lines are the cumulative rms. For the optimal control result, we also show its displacement and sensing noises in the dotted lines.



(a) Tolerance on the fractional drifts of the arm power. (b) Tolerance on the fractional variation in the sensing gain.

Figure 9: Robustness of the optimal controller for the hard mode. We have assumed the nominal arm power of $P_{\text{arm}} = 0.75 \text{ MW}$. The bounds are obtained from the small gain theorem and thus they are sufficient conditions (i.e. conservative estimations) for loop stability.

A H_∞ - AND μ -SYNTHESES

. Loosely speaking, the H_∞ problem can be stated as the following:

- Given a plant P , the algorithm tries to find a controller K such that
 - the controlled feedback is stable.
 - the ∞ -norm³ of the closed-loop transfer matrix $H = [W_1 S, W_2 T]^T$ is minimized, with $\|H\|_\infty = \gamma$ for some $\gamma > 0$. Here $S = (1 + PK)^{-1}$ (which characterizes the low-frequency suppression) and $T = PK(1 + PK)^{-1}$ (which characterizes the high-frequency roll-off), and W_1 and W_2 are frequency-dependent weights input by the user.

For a single-input-single-output (SISO) problem the second point can be translated to

$$|W_1(i\omega)S(i\omega)|^2 + |W_2(i\omega)T(i\omega)|^2 = \gamma^2. \quad (8)$$

Since $S = (1 + PK)^{-1}$ is important at low frequencies and $T = PK(1 + PK)^{-1}$ important at high frequencies, we can further write

$$|W_1(i\omega)S(i\omega)| \simeq \gamma, \text{ for small } \omega, \quad (9)$$

$$|W_2(i\omega)T(i\omega)| \simeq \gamma, \text{ for large } \omega. \quad (10)$$

Furthermore, at low frequency we should have $PK \gg 1$ (i.e., $S \simeq 1/PK$) and high frequency $PK \ll 1$ (i.e., $T \simeq PK$), which leads to

$$|PK| \simeq \frac{1}{\gamma} |W_1|, \text{ for small } \omega, \quad (11)$$

$$|PK| \simeq \gamma \frac{1}{|W_2|}, \text{ for large } \omega. \quad (12)$$

For properly set weights, $\gamma \sim \mathcal{O}(1)$. Thus by choosing the proper weighting functions $W_1(i\omega)$ and $W_2(i\omega)$, we can shape the open-loop transfer function PK to have the desired (asymptotical) frequency response, and the controller K to satisfy the target in the optimal way can be obtained in the H_∞ -synthesis process.

A subtlety arises when we including the effect of radiation torque. It modifies the plant as $P_{ss}(P_{\text{arm}}) = P_0/[1 + P_0 R(P_{\text{arm}})]$. Instead of the function⁴ $S_{ss} = (1 + KP_{ss})^{-1}$, what we are really interested in is the closed-loop torque-to-angle transfer function $P_{ss}/(1 + KP_{ss}) = P_{ss}S_{ss}$. Specifically, we want

$$P_{ss}S_{ss} = P_0S_0 = \text{constant}, \quad (13)$$

where we have used S_0 to denote the S function at zero arm power. Therefore we should modify the weighting function $W_1 = W_1(P_{\text{arm}})$ as

$$W_1(P_{\text{arm}}) = \frac{W_{1,0}}{1 + P_0 R(P_{\text{arm}})}, \quad (14)$$

³the largest singular value across frequencies

⁴Note that $KP_{ss} \neq OL = (R + K)P_0$. Thus this quantity does not preserve the torque-to-torque open loop function. Nonetheless, the closed-loop torque-to-angle response is preserved, as $P_{ss}/(1 + KP_{ss}) = P_0/[1 + (K + R)P_0]$.

where $W_{1,0}$ is the weight in the free pendulum limit.

In Fig. 10 we show the weighting functions $W_{1,0}$ and W_2 used in our design. At low frequencies we want as large gain as possible, with some extra emphasize on the microseismic peak at around 0.5 Hz (also close to the main suspension resonance). At high frequencies, on the hand, we want the sensing noise to roll-off as fast as possible. The H_∞ -synthesis algorithm finds the optimal controller satisfying (or trying to satisfy) those requirements while guaranteeing the internal stability. The settings already yield better performance than the current ASC design, yet can be further improved in the future studies.

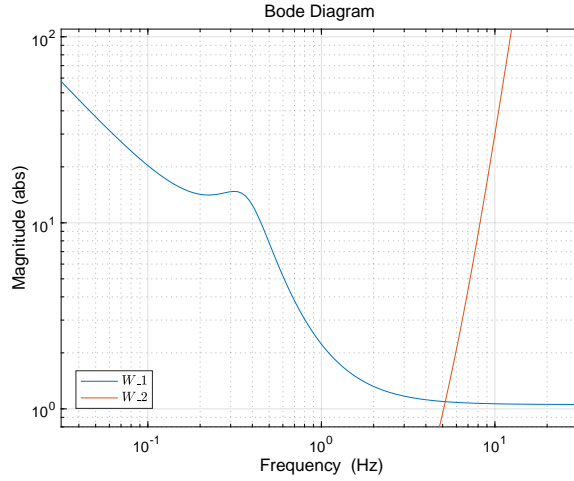


Figure 10: The weighting functions $W_{1,0}$ (blue trace; zero power limit, cf. Eq. 14) and W_2 used in the design. At low frequencies $|W_1| \simeq$ the loop suppression of the input displacement noise, while at high frequencies $1/|W_2| \simeq$ the roll-off of the sensing noise.

The controller designed via H_∞ -synthesis, while optimal in the frequency response, may not be robust against uncertainties or perturbations to the the plant. Therefore controllers presented in this note are actually calculated based on the μ -synthesis. Approximately speaking, it can be viewed as an extension of the H_∞ -synthesis with the plant P now being a system with some uncertainty; otherwise it is sufficiently similar to the H_∞ -synthesis.

Lastly, standard Matlab packages exists for the optimal control. The optimal controller can be easily obtained using `hinfsyn` for H_∞ -synthesis and `dksyn` for μ -synthesis. Improving the control performance can thus be translated into the (much simplified) exercise of optimizing the weighting functions.

B THE SMALL GAIN THEOREM AND THE CONTROLLER ROBUSTNESS

The small gain theorem can be a useful tool for studying the stability of a feedback system. In a not-so-mathematically-rigorous way, it can be stated as the following:

- Suppose that a feedback system has an open-loop gain L , then a *sufficient* condition for it to be internally stable is that

$$\|L\|_\infty < 1. \quad (15)$$

This allows us to decompose the system as $L = H\Delta H$, with H being the nominal part (including plant and controller) and ΔH being a perturbation. Then the small gain theorem implies that a sufficient condition for stability of the perturbed system is

$$\|H\Delta H\|_\infty \leq \|H\|_\infty \cdot \|\Delta H\| < 1, \quad (16)$$

$$\text{or } \|\Delta H\|_\infty < \frac{1}{\|H\|_\infty}. \quad (17)$$

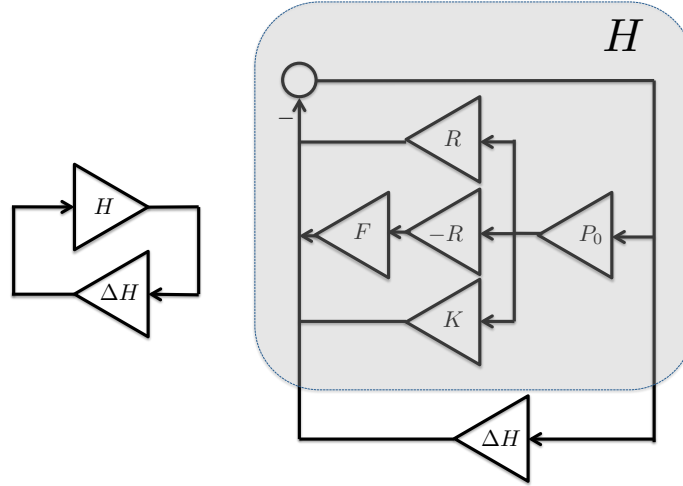


Figure 11: Left: the basic perturbation model. H is the nominal system (both plant and controller) and ΔH is some perturbation. From the small gain theorem a sufficient condition for the loop to be stable is the $\|\Delta H\|_\infty < 1/\|H\|_\infty$. Right: applying the basic perturbation model to the ASC system. Combining the elements in the shaded region leads to $H = -1/[1 + (R - FR + K)P_0]$, which can be used to derive tolerance on the perturbation term ΔH .

It can be applied to the ASC system as shown in Fig. fig:pertModel. The nominal torque-to-torque transfer function H can be written as

$$H = \frac{-1}{1 + (R - FR + K)P_0} = \frac{-1}{1 + OL}, \quad (18)$$

which can be translated to a tolerance on the torque-to-torque perturbation ΔH as

$$\|\Delta H\|_\infty < \|1 + (R - FR + K)P_0\|_\infty. \quad (19)$$

In the study of the soft mode robustness, we have treated the perturbation as due to imperfect subtraction, with

$$\Delta H = \Delta FR_s P_0. \quad (20)$$

Then Eq. (19) can be converted into a tolerance on ΔF , with the result shown in Fig. 5. If ΔF is flat across frequency (which is likely to be the case as we only need to set a DC gain for the digital subtraction path), then it is sufficient to maintain the perturbed loop's stability if $|\Delta F|$ is smaller than the minimum of the curve shown in Fig. 5. Even the estimation is quite conservative, we can see that the controller can handle 60% gain mismatch in the subtraction path.

In addition to the modeled perturbation, we can use the small gain theorem to derive tolerances on less well understood perturbations like the $dP/d\theta$ instability (which is known phenomenologically yet a complete analytical modal is yet to be developed). Since most perturbations are likely to couple with the suspension system, we plot the tolerance on $\Delta H/P_0$, or effectively, $\|(1 + K_s P_0)/P_0\|_\infty$ in Fig. 12. Note that the most vulnerable frequencies to perturbations are the suspension resonant frequencies (0.5 Hz and 1.5 Hz). These are consistent with the observed frequencies of instabilities. If in reality the instability happens, the weight in W_1 can be increased at the corresponding frequencies.

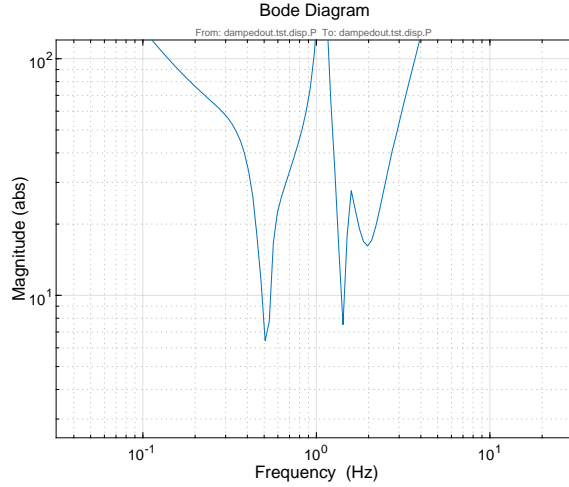


Figure 12: Tolerance on the unstructured angle-to-torque perturbation, i.e., the quantity $\|(1 + K_s P_0)/P_0\|_\infty$. It can be used to estimate the tolerance on less well-understood perturbations including the $dP/d\theta$ instability.

Similar robustness analysis can be applied to the hard mode as well. Here we consider two types of torque-to-torque perturbations. The first one is due to power drift in the arms. It changes the amount of the SS feedback, which can be viewed as a perturbation term of

$$\Delta H^{(dP_{\text{arm}})} = \frac{dP_{\text{arm}}}{P_{\text{arm}}} R_h P_0. \quad (21)$$

The second type is due to the drift in the sensing gain, which changes the controller strength and perturbs the plant by

$$\Delta H^{(dK)} = \frac{dK}{K} \Big|_{\text{DC}} K P_0. \quad (22)$$

Plugging each ΔH back to Eq. 19 allows us to compute the conservative tolerance on $(dP_{\text{arm}}/P_{\text{arm}})$ and $(dK/K)_{\text{DC}}$, respectively. The results are summarized in Fig. 9. The

controller can maintain loop stability for $\lesssim 15\%$ power drift or $\lesssim 20\%$ variation in the sensing gain. Those values are within the typical fluctuation for a long lock stretch and thus the controller is not only optimal in the noise performance but also robust under perturbations.